Nanoscaffold's stiffness affects primary cortical cell network formation

Sijia Xie[a] and Bart Schurink
Mesoscale Chemical Systems, MESA+ Institute for Nanotechnology, University of Twente, 7500 AE Enschede, The Netherlands

Floor Wolbers and Regina Luttge[b]
Mesoscale Chemical Systems, MESA+ Institute for Nanotechnology, University of Twente, 7500 AE Enschede, The Netherlands and Department of Mechanical Engineering, Microsystems Group and ICMS Institute for Complex Molecular Systems, Eindhoven University of Technology, 5612 AZ Eindhoven, The Netherlands

Gerco Hassink
Department of Biomedical Signals and Systems, MIRA Institute for Biomedical Technology and Technical Medicine, University of Twente, 7500 AE Enschede, The Netherlands

(Received 27 June 2014; accepted 14 October 2014; published 27 October 2014)

Networks of neurons cultured on-chip can provide insights into both normal and disease-state brain function. The ability to guide neuronal growth in specific, artificially designed patterns allows us to study how brain function follows form. Primary cortical cells cultured on nanograting scaffolds, in particular astrocytes, showed highly ordered regions of dendritic outgrowth. Usually, materials suitable for nanopatterning have a stiffness far above that of the extracellular matrix. In this paper, the authors studied two materials with large differences in stiffness, polydimethylsiloxane (PDMS) and silicon. Our results show that both nanopatterned silicon and PDMS guide the outgrowth of astrocytes in cortical cell culture, but the growth of the astrocyte is affected by the stiffness of the substrate, as revealed by differences in the cell soma size and the organization of the outgrowth. [http://dx.doi.org/10.1116/1.4900420]

I. INTRODUCTION

Cells are sensitive to the mechanical properties of their environment. In tissue, the extracellular matrix (ECM) influences the function of neuronal cells, providing not only a physical scaffold, but also chemical cues for cell growth and behavior.[1] Properties such as the stiffness and topography of the scaffold material have a significant effect on the number of primary neurons and astrocytes attached, as well as on the direction of their outgrowths.[2–4] Researchers have been working on micro- or nanopatterned substrates to guide neuronal outgrowth, to help study the neural electrical signal transmission in single neurons,[5] and to aid nerve regeneration processes.[6] Therefore, our goal is to combine microfluidics with tissue engineering to create a "living brain," generating realistic *in vitro* neural circuitry, which can be used to standardize experimental neuronal cell culture.[7] Networks of neurons cultured on-chip can provide insights into both normal and disease-state brain function. The ability to guide neuronal growth in specific, artificially designed patterns allows us to study how brain function follows form.

The mechanical properties of an artificial substrate or scaffold play an important role in cell culturing. In this context, researchers have investigated different gel-type substrates and measure the stiffness of the cortex tissue.[2,8] For example, Norman and Aranda-Espinoza used atomic force microscopy (AFM) to measure the Young's modulus of the fetal rat's cortex, resulting in values of around 305 Pa.[8] It was reported that the primary astrocytes showed different cell morphology[2] and different foreign body reactions[9] on gel matrices that with different stiffnesses. Primary neurons, however, no matter cultured alone or in mixture with glial cells, did not show distinct morphological difference on gels with varies stiffness, but showed different viability rates—lower stiffness led to a higher viability.[2] However, materials suitable for nanopatterning by microelectromechanical system (MEMS) technology, like silicon and polydimethylsiloxane (PDMS), have a stiffness far above that of the cortical ECM (Table I). Hence, we investigated in this paper the effect of these two materials on astrocytes in primary cortex. The observation of differences on these stiffer substrates will help us to optimize the artificial environment for *in vitro* analyzing system on chip.

In our previous work, we demonstrated that cultures of primary cortical cells were sensitive to the specific nanoscale surface structure on silicon with a nanoimprinted groove-scaffold of resist. Cortical cells grown on such nanogroove scaffolds with periods between 400 and 600 nm and a height of 118 nm, showed highly ordered regions of outgrowth with a preferential alignment tendency for astrocytes.[10]

Here, we study two materials with large differences in stiffness, PDMS and silicon. The Sylgard 184® PDMS is widely used in micro- or nanochips[11] for biological studies, due to its advantages such as high transparency, good biocompatibility, gas permeability, low autofluorescence, and its easy fabrication process by replication. Furthermore, nanopatterned PDMS has already been used to show the differentiation of mesenchymal stem cells toward the neuronal lineage.[12] On the other hand, silicon is a well-established material in nanoelectromechanical system and MEMS. Micro- and nanopatterned silicon has been used as substrate for *in vitro* studies in tissue engineering.[13,14] What's more, due to the high levels of integration possible in silicon, it is

[a]Electronic mail: s.xie@utwente.nl
[b]Electronic mail: r.luttge@tue.nl

TABLE I. Estimates of the Young's moduli of PDMS with different mixture ratio (n = 3).

Ratio of prepolymer and curing agent	Young's modulus (MPa)	Valu e from the literature (Ref. 21) (MPa)
10:1	1.113 ± 0.109	1.167 ± 0.088
20:1	0.246 ± 0.012	0.397 ± 0.019
40:1	0.039 ± 0.002	0.078 ± 0.008

used for advanced laboratory-on-a-chip systems, enabling the study of cells within microfluidic devices, leading to proposals for organs-on-a-chip.[15] Although silicon microfabrication processes are straightforward and capable of delivering high fidelity patterns down to the nanoscale region, and can thus be used to create nanostructured surfaces suitable for organ-on-chip technology, it is not clear whether silicon's mechanical properties are such that realistic cell morphologies will form. Our results show that, while both nanopatterned silicon and PDMS scaffolds guide the outgrowth of astrocytes in primary cortical culture, the astrocytes on the softer PDMS substrates formed smaller soma size and a denser soma distribution than on the harder silicon ones. Additionally, we studied the astrocytes' morphology on flat PDMS substrates with different stiffnesses, and found that the astrocytes continue to exhibit soma sizes that decrease with decreasing scaffold stiffness, and the soma size on less stiff substrate is getting closer to the *in vivo* staining results.[16] We thus hypothesize that astrocytes' response to the nanoscaffold's stiffness, may have a profound effect on neuronal network formation. Further, the ability to tune the nanoscaffold's stiffness will help us to find an approach to creating more realistic *in vitro* neuronal network models in the future.

II. EXPERIMENT

A. Nanoscaffolds

The silicon nanoscaffolds [Fig. 1(b)] were fabricated by reactive ion etching using an in-house build dry-etch equipment (MESA + Institute for Nanotechnology, University of Twente) of resist scaffolds [Fig. 1(a)] formed by jet and flash imprint lithography (J-FIL™) on silicon substrates. Materials and the fabrication process details are described in our previous work.[10] In brief, the patterning process contains the following steps: first dispensing and imprinting of nonsilicon Monomat using the Imprio55 equipment (Molecular Imprints Inc., USA) and subsequently transferring the resist scaffold into silicon by CHF_3:SF_6:O_2 gas composition at 60 W for 1 min 40 s. The soft nanoscaffolds [Fig. 1(c)] were fabricated by PDMS (Sylgard 184, Dow Corning) soft lithography,[17] using the imprinted resist nanoscaffolds on silicon substrates as templates [Fig. 1(a)].

B. Flat substrates

The flat silicon surface [Fig. 1(d)] was cut from a polished (100) silicon wafer, serving as the "stiff" substrate, with a Young's modulus around 130 GPa (100 direction) and 169 GPa (110 direction), according to the literature.[18] We prepared a series of flat PDMS substrates with ratios of prepolymer and curing agent of 10:1, 20:1, and 40:1, respectively, by pouring a layer of polymer mixture of around 1 mm thickness onto a clean polished silicon wafer, and curing the PDMS at 80 °C for 1.5 h after degassing in a vacuum chamber. The cured PDMS was peeled from the silicon wafer and cut into 9 × 9 mm pieces. The surface that contacted with the silicon wafer was used for cell seeding [Fig. 1(e)].

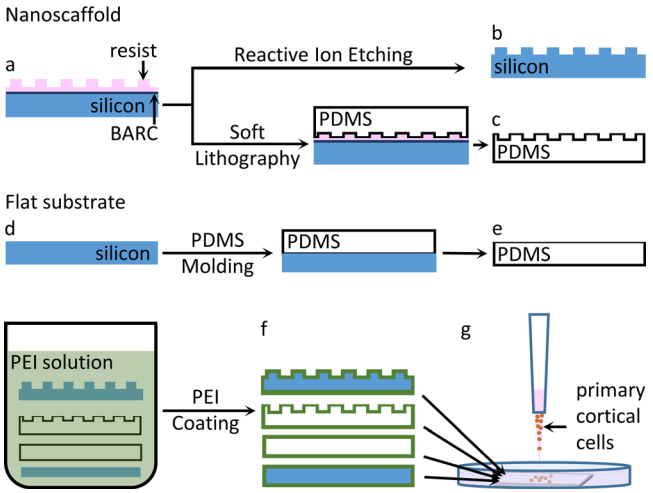

FIG. 1. (Color online) Fabricating of the substrates for cortical culture. (a) imprinted resist scaffold by J-FIL imprinting; (b) silicon scaffold realized by RIE pattern transfer from (a); (c) replicated PDMS scaffold using (a) as a template; (d) flat silicon substrate; (e) flat PDMS peeled from the silicon substrate; (f) PEI coated substrates (b)–(e); and (g) culture of primary cortical cells on top of PEI coated substrates.

In order to improve cell adhesion and viability, all these substrates and scaffolds were coated with polyethylenimine (PEI) by being immersed in a branched PEI (approx. M.N. 60000, 50 wt. % aq. solution, Acros Organics, CAS: 9002–98-6) solution with a concentration of 50 μg/ml in sterile milliQ water at 37 °C overnight. The redundant coating solution was removed from the nanoscaffolds the next day. The coated substrates [Fig. 1(f)] were then air-dried in a biological safety cabinet before being ready for cell seeding [Fig. 1(g)].

C. Primary cortical cell culture

The primary cortical cells were isolated from a new born rat's cortex and were applied on top of the PEI coated flat substrates and nanoscaffolds in a standard 24 well culturing plate (Corning® Costar®), at a density of 4000–4500 cells/μl for approximately 2 h. Hereafter cells were maintained in R12H medium[19] supplemented with penicillin/streptomycin antibiotics at 37 °C, 70%–80% relative humidity and 5% CO_2 and were refreshed every two days until analysis.

D. Immunostaining

To study the behavior of astrocyte in the primary cortical cell culture, we performed immunostaining using astrocyte specific anti-GFAP antibody (goat; Sigma, SAB2500462; 1:200) as primary antibody, and antigoat IgG (H + L), CF™

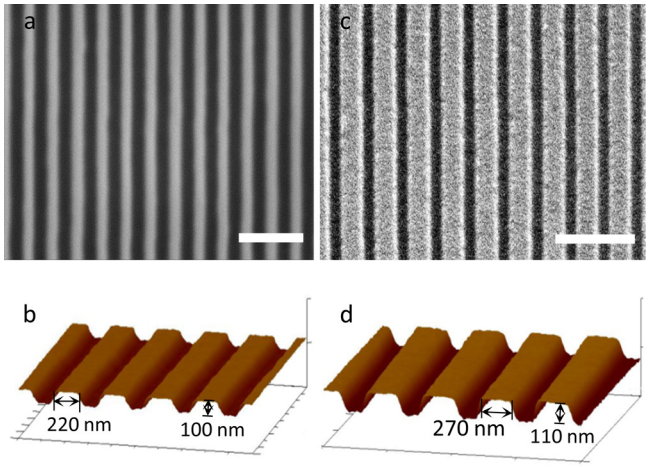

FIG. 2. (Color online) Structure of the nanoscaffolds, taking one silicon scaffold and one PDMS scaffold as examples. (a) and (c) SEM images of the top view of the silicon scaffold (a) and the PDMS scaffold (c). Scale bar: 1 μm; (b) and (d) AFM 3D images of the silicon scaffold (c) and the PDMS scaffold (d).

488A (donkey; Sigma Aldrich, SAB4600032; 1:200) as the secondary antibody. The staining protocol followed the standard protocol by Yale Center for high throughput cell biology.[20]

E. Microscopy

We used AFM (Bruker ICON) and scanning electron microscopy (SEM; JEOL5610, JEOL USA, Inc.) to characterize the structure of the nanoscaffolds. AFM data were recorded and depicted as 3D models with Nanoscope 8.15 software (Bruker Corporation). To observe and image the staining of the cells, we used optical fluorescence microscopy (Leica, DMI5000M) and then analyzed the images with the Leica application suite software (Leica Microsystems, LAS05160).

F. Statistical analysis

We performed the statistical analysis with the help of ImageJ (National Institute of Health, USA) for calculating the area of the cells. The Eroding and Dilating function in binary process helped to show the soma of the cell, and the Analyze Particles function calculated the area of the soma.

III. RESULTS AND DISCUSSION

A. Young's modulus of the PDMS surfaces

The Young's moduli, E, of the PDMS samples were determined by a uniaxial tensile test.

PDMS shows a nonlinear stress–strain curve, so we calculate E based on the initial, linear portion of the data. The results are summarized in Table I.

B. Geometrical characterization of the nanoscaffolds

Figure 2 depicts the structure of the nanoscaffolds. To avoid confounding the effects of substrate stiffness on cell behavior with other variables, we chose samples of the different materials with topographies that were as similar as possible. The period width (P) of the stiff silicon scaffold [Figs. 2(a) and 2(b)] was around 400 nm, the ridge width (R) around 220 nm, and the height of the ridge (H) around 100 nm, while for the PDMS scaffold [Figs. 2(c) and 2(d)] P was around 450 nm, R around 270 nm, and H around 110 nm. The SEM images [Figs. 2(a) and 2(c)] give a top

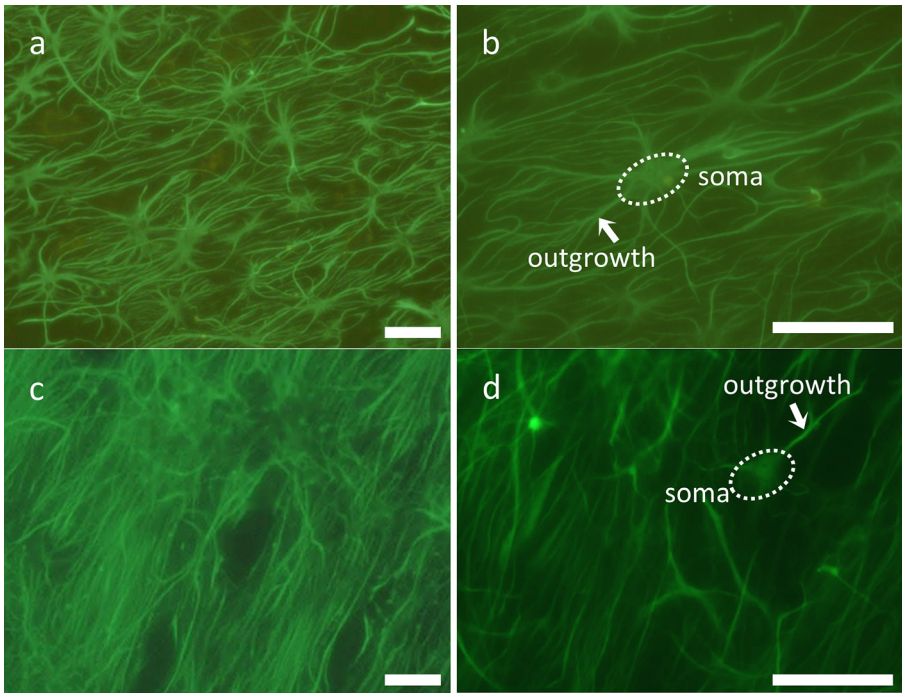

FIG. 3. (Color online) Morphology of the astrocyte outgrowth on nanoscaffolds with different stiffness. (a) and (b) silicon scaffolds; (c) and (d) 10:1 PDMS scaffolds. Scale bar: 50 μm.

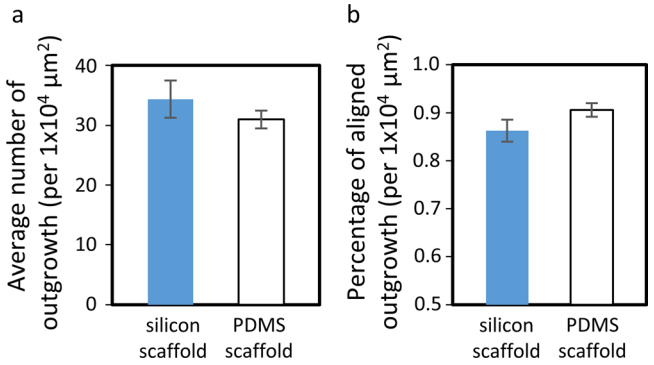

FIG. 4. (Color online) Statistical comparison of the astrocyte outgrowth on nanoscaffolds that with different stiffness. (a) Average number of the astrocyte's outgrowth per 100 × 100 μm (n = 8); (b) Average percentage of aligned outgrowth per 100 × 100 μm. The "aligned outgrowth" is defined as a deviation of the direction of the grooves within an angle of less than ±30° (n = 8).

view of the nanogrooves. The AFM 3D models [Figs. 2(b) and 2(d)] show the profile and the surface of these scaffolds.

C. Cell immunostaining

We compared the morphology of the astrocyte outgrowth on the grooved nanoscaffolds with different stiffnesses. Figures 3(a) and 3(b) are the immunostaining images of the astrocytes on stiff silicon nanoscaffolds, while Figs. 3(c) and 3(d) are the astrocytes on the softer 10:1 PDMS nanoscaffolds. With the same seeding density and surface modification, the outgrowths of the astrocytes showed a different organization on the PDMS scaffolds (c), compared with those on the silicon scaffolds (a). The somas in (a) appear more evenly distributed over the image area than somas in (c), and by comparing astrocytes at a single soma level (d) and (b), astrocytes on PDMS are less spread. Figure 4 gives a comparison of the astrocytes' outgrowth formation within an area of 100 by 100 μm. These statistical data show no obvious difference between these two types of scaffolds, while the morphological change in Fig. 3 was distinct.

Figure 5 shows the cell morphology of single astrocytes grown on different flat substrates. Comparing these four pictures, there is a clear tendency for the soma size to decrease with decreasing substrate stiffness. The statistic comparison result (Fig. 6) confirms this tendency. The decrease of the soma size implies that the morphology of the astrocytes becomes more comparable to the *in vivo* staining results with a diameter of the soma size around 10 μm.[16]

In our previous work, we found that astrocytes align preferentially with the nanoscaffolds grooves in the primary cortical culture. Supported by the research of Wheeler *et al.* and Johansson *et al.*, it seems that the neuronal culture of neuron cell lines and nerves with nanogrooved substrates exhibited obvious neuronal outgrowth alignment.[5,22] Recently, the function of astrocytes has attracted more interest in neurosciences. Astrocytes play a biochemical supporting role for neurons in the blood–brain barrier, help with the nutrient transport, and also perform chemical signal transmission, such as calcium ion-dependent transmitter, to simulate and regulate the neuronal network of the brain tissue.[23] Astrocytes are also considered as a soft substrate for neurons' adhesion or support neuronal branching when the mixture of the brain cells grow on a far stiffer environment *in vitro* compared with the brain itself.[24] In addition, the synaptic transmission of neurons can also be affected by the surrounding astrocytic environment, such as the coverage of astrocytes.[25] Consequently, we suggest that the response of

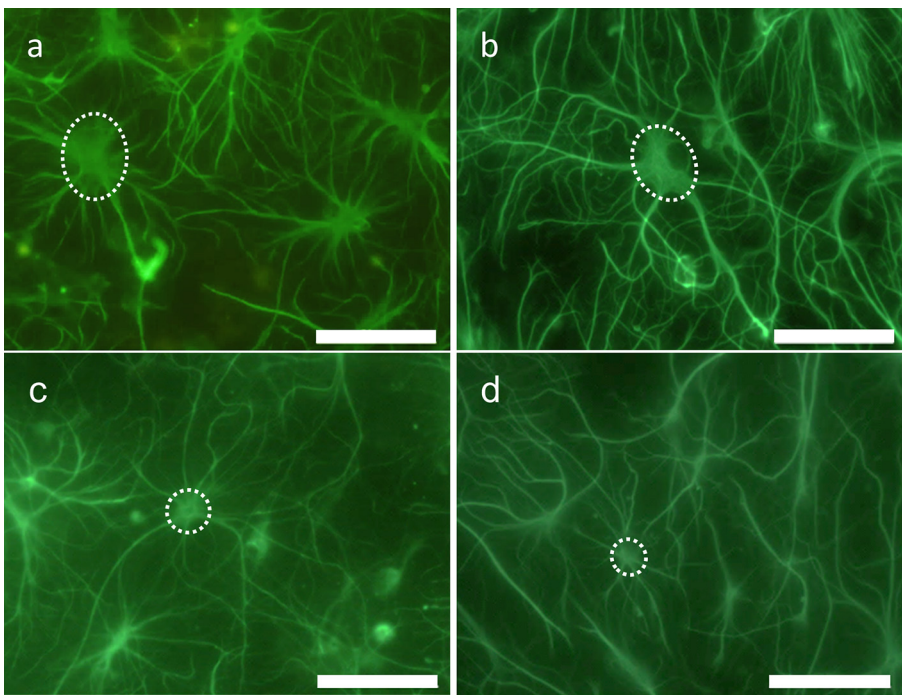

FIG. 5. (Color online) Morphology of a single astrocyte on flat substrates with different stiffness. (a) silicon; (b) 10:1 PDMS; (c) 20:1 PDMS; and (d) 40:1 PDMS. The white dashed circle points out the cell soma. Scale bar: 50 μm.

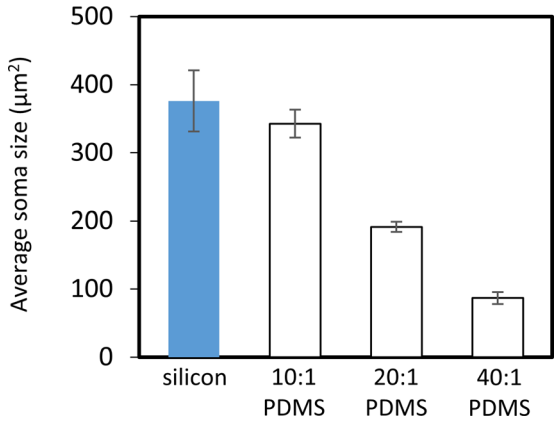

FIG. 6. (Color online) Statistical comparison of the average astrocyte's soma size on substrates with significant difference in stiffness (n = 7 for each substrate).

astrocytes to the stiffness of the scaffolds will profoundly influence the formation of the neuronal network that, in turn, is closely related to electrical signal transmission among the neurons. Ultimately, this is crucial for the normal functioning of the neuronal network. To better understand how the neuronal network will be affected by the organization of the nanoscaffolds and the supporting cells, such as astrocytes, a more detailed investigation of neuronal cell morphology in primary cortical cultures and electrophysiological recording studies are required in our future research.

IV. CONCLUSIONS

We have studied the cell morphology of the astrocyte in the primary cortical culture, comparing the effects of different substrate stiffness. We prepared PDMS substrates with a variety of stiffnesses by using different prepolymer to curing agent ratios, and introduced silicon substrate as a much stiffer material as a baseline. Our results indicated that the stiffness of the substrates can affect the growth of the astrocytes' soma size as well as their outgrowth formation. A better understanding of the stiffness effect in combination with the outgrowth guidance effect of the nanoscaffolds gives us more clues to further elucidate the formation of neuronal networks in cultured microsystems.

ACKNOWLEDGMENTS

This project was financially supported by the ERC, Grant No. 280281 (MESOTAS). The authors sincerely thank B. Vratzov (MESA + Institute) for assisting in J-FIL, and B. Klomphaar for providing dissociated cells (MIRA Institute). The authors thank J. G. E. (Han) Gardeniers for the helpful suggestion in the early preparation of this manuscript. For constructive comments on earlier versions of this article, the authors thank J. A. Liddle at the Center for Nanoscale Science and Technology at the National Institute of Standards and Technology, Gaithersburg, MD, USA.

[1]K. Franze, P. A. Janmey, and J. Guck Annu. Rev. Biomed. Eng. **15**, 227 (2013).
[2]P. C. Georges, W. J. Miller, D. F. Meaney, E. S. Sawyer, and P. A. Janmey Biophys. J. **90**, 3012 (2006).
[3]E. S. Ereifej, H. W. Matthew, G. Newaz, A. Mukhopadhyay, G. Auner, I. Salakhutdinov, and P. J. VandeVord J. Biomed. Mater. Res., Part A **101A**, 1743 (2013).
[4]L. M. Y. Yu, N. D. Leipzig, and M. S. Shoichet Mater. Today **11**, 36 (2008).
[5]J. M. Peyrin *et al.*, Lab Chip **11**, 3663 (2011).
[6]S. B. Elke, A. Bremus-Koebberlinga, B. Koch, and A. Gillner, J. Laser Appl. **24**, 042013 (2012).
[7]B. C. Wheeler and G. J. Brewer Proc. IEEE **98**, 398 (2010).
[8]L. L. Norman and H. Aranda-Espinoza Cell. Mol. Bioeng. **3**, 398 (2010).
[9]P. Moshayedi, G. Ng, J. C. F. Kwok, G. S. H. Yeo, C. E. Bryant, J. W. Fawcett, K. Franze, and J. Guck Biomaterials **35**, 3919 (2014).
[10]S. Xie and R. Luttge Microelectron. Eng. **124**, 30 (2014).
[11]Y. Shin, S. Han, J. S. Jeon, K. Yamamoto, I. K. Zervantonakis, R. Sudo, R. D. Kamm, and S. Chung Nat. Protoc. **7**, 1247 (2012).
[12]E. K. F. Yim, S. W. Pang, and K. W. Leonga Exp. Cell Res. **313**, 1820 (2007).
[13]A. M. Turner, N. Dowell, S. W. Turner, L. Kam, M. Isaacson, J. N. Turner, H. G. Craighead, and W. Shain J. Biomed. Mater. Res. **51**, 430 (2000).
[14]M. Ni, W. H. Tong, D. Choudhury, N. A. A. Rahim, C. Iliescu, and H. Yu Int. J. Mol. Sci. **10**, 5411 (2009).
[15]C. Moraes, C. Mehta, S. C. Lesher-Perez, and S. Takayama Ann. Biomed. Eng. **40**, 1211 (2011).
[16]F. Appaix *et al.*, PLoS One **7**, e35169 (2012).
[17]D. Qin, Y. Xia, and G. M. Whitesides Nat. Protoc. **5**, 491 (2010).
[18]M. A. Hopcroft, W. D. Nix, and T. W. Kenny J. Microelectromech. Syst. **19**, 229 (2010).
[19]H. J. Romijn, F. van Huizen, and P. S. Wolters Neurosci. Biobehav. Rev. **8**, 301 (1984).
[20]See: http://www.sigmaaldrich.com/content/dam/sigma-aldrich/docs/Sigma/General_Information/1/yale-if-procedure.pdf.
[21]N. Eroshendo, R. Ramachandran, V. K. Yadavalli, and R. R. Rao, J. Biol. Eng. **7**, 7 (2013).
[22]F. Johansson, P. Carlberg, N. Danielsen, L. Montelius, and M. Kanje Biomaterials **27**, 1251 (2006).
[23]T. A. Fiacco, C. Agulhon, and K. D. McCarthy Annu. Rev. Pharmacol. **49**, 151 (2009).
[24]D. E. Discher, P. Janmey, and Y. Wang Science **310**, 1139 (2005).
[25]R. Piet, L. Vargova, E. Sykova, D. A. Poulain, and S. H. R. Oliet Proc. Natl. Acad. Sci., U. S. A. **101**, 2151 (2004).